Clinical Application of Dual-Source Dual-Energy CT in Children

Jing Qi, MD, Eric Eutsler, MD, and Marilyn Siegel, MD

Pediatric Radiology, Mallinckrodt Institute of Radiology
Washington University School of Medicine
St. Louis, MO

MIR Mallinckrodt Institute of Radiology

Washington University in St. Louis
School of Medicine

Methods & Materials

- Descriptive, retrospective study.
- Dual-source, dual-energy CT (DECT) studies performed at our institution over the last two years were reviewed.
- Case examples of the common post-processing algorithms and their clinical application in pediatric patients are presented.

DECT Protocol

- Dual-source energy: 80kV and Sn-140 kV (Sn indicates tin pre-filtration)
- Collimation: 128 × 0.6 mm
- Pitch: 1.2
- Rotation time : 0.28 seconds

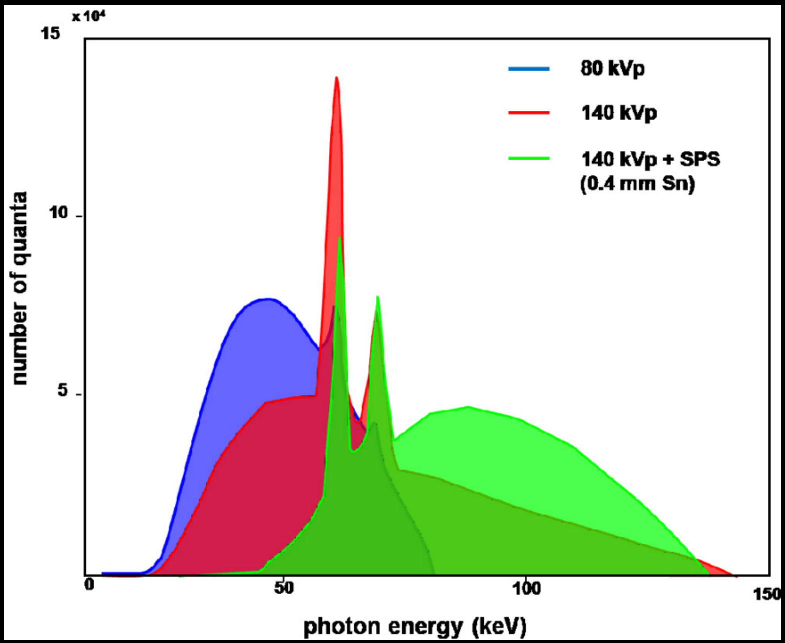

From: Johnson TRC. *Physics of Dual Energy CT.*

- Each tube produce polychromatic spectra from Bremsstrahlung effect
- Tin filter eliminates low-energy quanta, improving spectra separation

Scan Parameters: DECT vs SECT

Parameter	Dual-Energy CT	Single-Energy CT
Collimation (mm)	128 × 0.6	128 × 0.6
Pitch	1.2	3.0
Rotation time (s)	0.285	0.285
Automatic exposure control	Yes	Yes
Tube potential (kVp)	Tube A, 80; tube B, 140Sn	70–120 kV, selected automatically according to patient size and indication
Automated tube potential selection (CARE kV, Siemens Healthcare)	NA	Yes; set up as follows: 120 kV as reference voltage; unenhanced, position 3; enhanced, position 7; angiography, position 11
Quality reference tube current–time product (mAs)[a]	150 (thoracic, contrast-enhanced)	110 (thoracic contrast-enhanced, CTA)
	125 (CTA)	150 (thoracic-abdominal-pelvic)
	275 (unenhanced and contrast-enhanced abdominal-pelvic)	180 (unenhanced and contrast-enhanced abdominal-pelvic)
	250 (thoracic-abdominal-pelvic)	
Reconstruction kernel	Medium smooth	Medium smooth
Reconstruction algorithm	Q30	I30
Slice thickness/interval (mm)	3/3	3/2

Note—Sn = tin filtration, NA = not applicable, CTA = CT angiography.
[a]Corresponds to tube A; value for tube B is automatically set by the scanner and is not shown in table.

Table used with permission. Siegel MJ et al. *AJR.* 2016.

Radiation Exposure of DECT

- DECT has been shown to be *dose neutral* to SECT in children
- Selective Photon Shield (Sn filter) blocks low-energy photons from the high-energy source and prevents unnecessary exposure

Size-Specific Dose Estimate (SSDE) in 79 children, DECT vs SECT

	Median SSDE
DECT	5.9 mGy
SECT	7.7 mGy

11.2% *reduction* in radiation exposure with DECT ($p < 0.01$)

Data used with permission. Siegel MJ et al. *AJR.* 2016.

Workflow

- Each acquisition produces 3 datasets:
  - 80 kV (relatively more contrast and more noise)
  - Sn-140 kV (relatively less contrast and less noise)
  - Blended dataset (default ratio: 0.5, or 50% contribution from each source; can use any ratio from 0.3 to 0.7)
- The default blended dataset has an appearance similar to traditional 120 kVp SECT images
- Any or all of the datasets may sent to the PACS according to radiologist preference

Workflow

- Additional post-processing is performed on a separate thin-client workstation depending on the clinical indication
  - For example, monoenergetic or material-specific images
- These images are then also sent to the PACS

DECT Post-processing Options

- *Virtual Monoenergetic (VM) Images:* VM reconstructions enable generation of an image with a single keV (40-190 keV)
  - Low keV images improve iodine contrast due to increased photoelectric absorption. The k-edge of iodine is 33.2 keV.
  - High keV images improve metal artifact by reducing beam hardening ("streak") effects
- *Material-selective Images*
  - Virtual Noncontrast
  - Lung Perfusion
  - Urinary Tract Stone Characterization
  - Automated Bone Subtraction

Virtual Monoenergetic (VM) Images

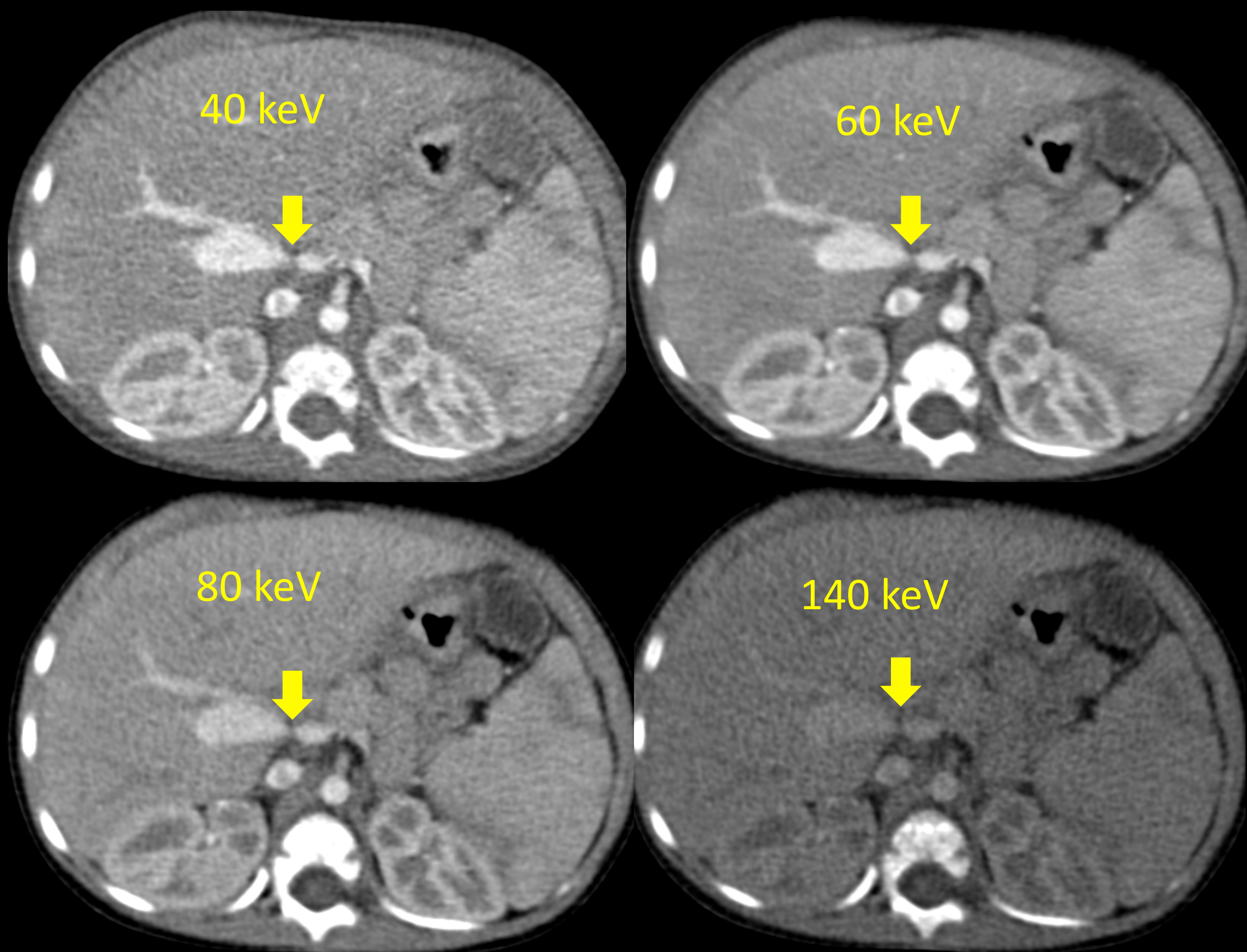

19-month-old male post liver transplant, with high grade stenosis of the main portal vein at the anastomosis (yellow arrow). Low keV image (40 keV) provides high contrast and high noise. High keV image (140 keV) offers a better noise profile, but compromises contrast. Intermediate energy images (60 keV, 80 keV) balance the contrast and noise.

Low Energy VM Images

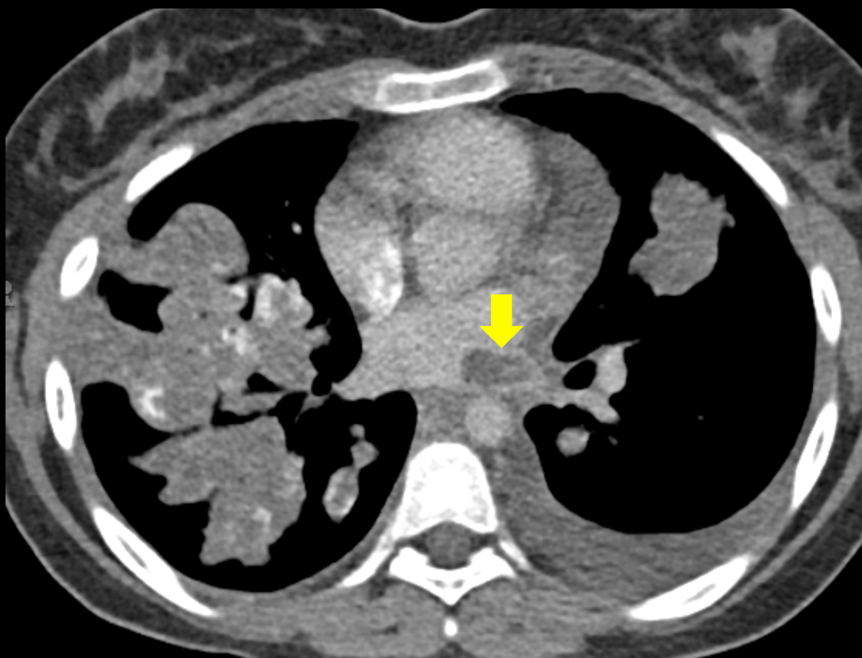

120 kVp

70 keV

17-year-old female with metastatic osteosarcoma. The left inferior pulmonary vein thrombus is better seen on the low energy VM image (yellow arrow).

High Energy VM Images

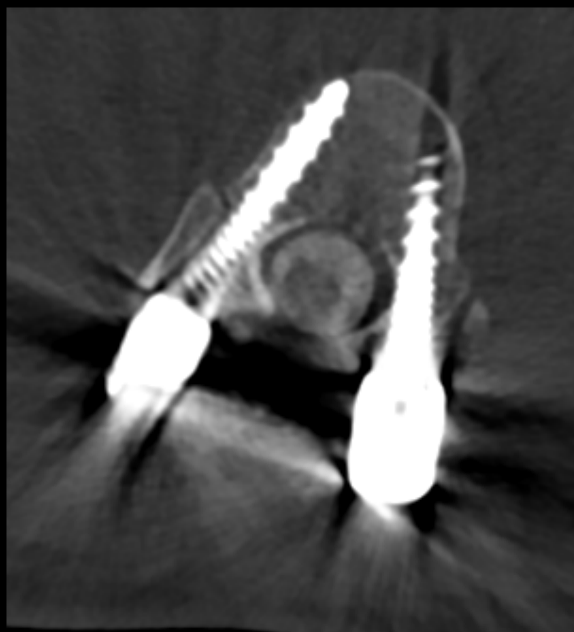

120 kVp

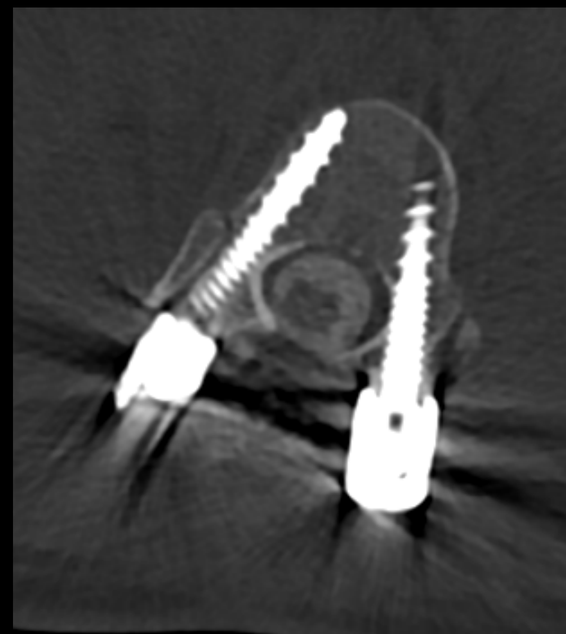

140 keV

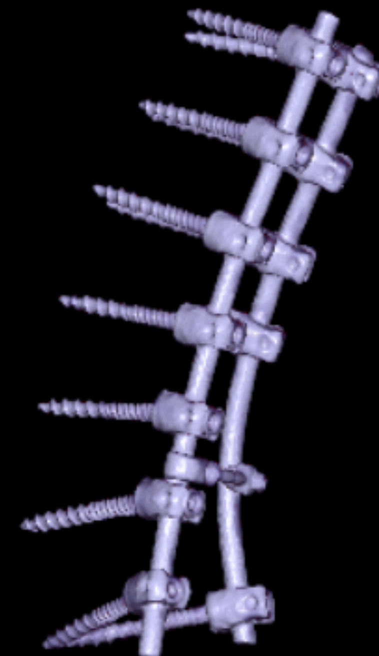

14 year old male with scoliosis status post instrumented posterior spinal fusion, presents with weakness. CT myelogram was performed. There is severe metal artifact with 120 kVp images, which improved on 140 keV VM images. The spinal cord is better delineated on VM images. SSD reconstruction shows the hardware is intact.

High Energy VM Images

140 kVp

140 keV

17-year-old male with Fontan-associated liver disease being evaluated prior to heart transplant. The patient has spine instrumentation causing substantial streak artifact that obscures the liver, even on the 140 kVp image. High energy VM images (140 keV) reduce the metal artifact and improves visualization of the liver, which showed no arterially-enhancing focal lesion.

Material-selective Images

- Materials have unique attenuation profiles at different energy levels according to their linear attenuation coefficient
  – Virtual Noncontrast Images (VNC; remove iodine or demonstrate Ca++)
  – Iodine Images (Lung Perfusion, Iodine Mapping)
  – Urinary Tract Stone Characterization
  – Automated Bone Removal
  – Simple creation of high quality 3D reconstructions

VNC: Remove Iodine

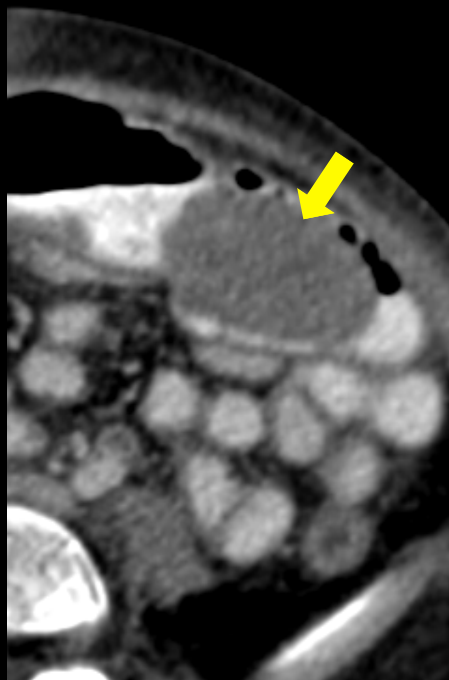

Blend (r=0.6)

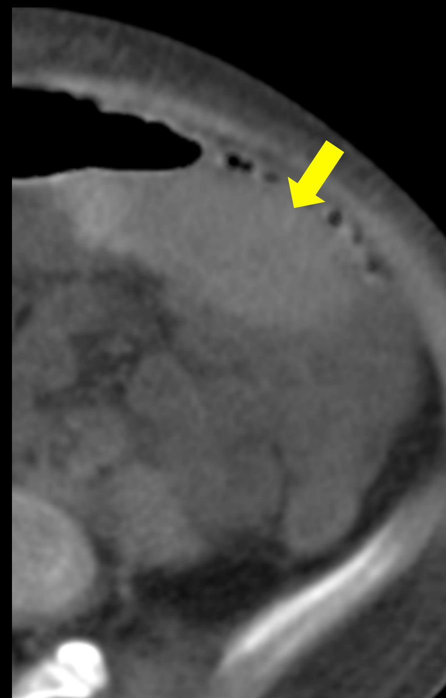

VNC

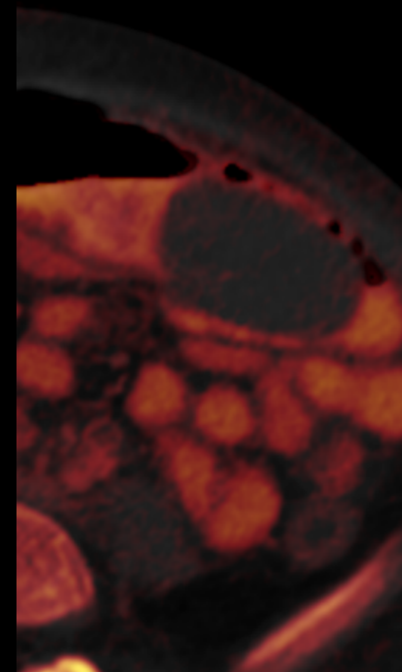

Iodine Map

7-year-old male with adrenal leukodystrophy, status post stem cell transplant complicated by bowel graft-versus-host disease and dropping hematocrit. On the blended image, there is an intraluminal mass in the jejunum (arrow). The VNC image demonstrates that the mass is hyperdense and the iodine map confirms no enhancement, consistent with a hematoma.

VNC: Demonstrate Ca++

80 kVp | 14 min delay | VNC

13-year-old male with a calyceal diverticulum and stone. It is difficult to evaluate renal stone on CT with contrast . Excretory phase image shows the cystic area communicating with pelvicalyceal system. VNC image confirms renal stone in the calyceal diverticulum (arrow). VNC obviates need for additional noncontrast image acquisition.

Lung Perfusion

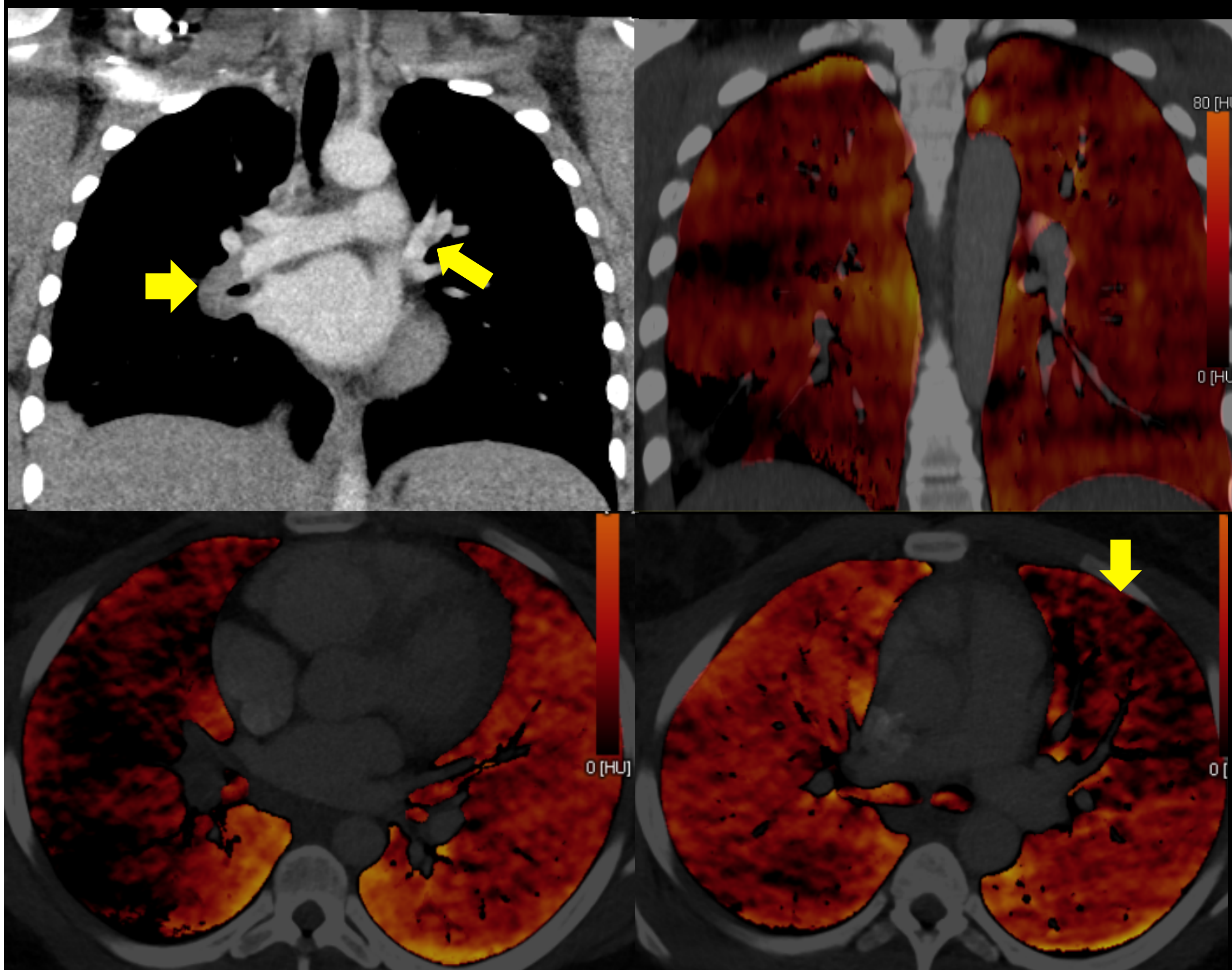

15 year old female with right upper quadrant pain.

- PE protocol demonstrates pulmonary embolism within the right interlobar artery (arrow).
- Lung perfusion images demonstrate decreased pulmonary blood volume of the right middle lobe and lower lobe.
- In addition, there is decreased perfusion to the left upper lobe. On further review, there is a small embolus in the left upper lobar artery.

Iodine Mapping

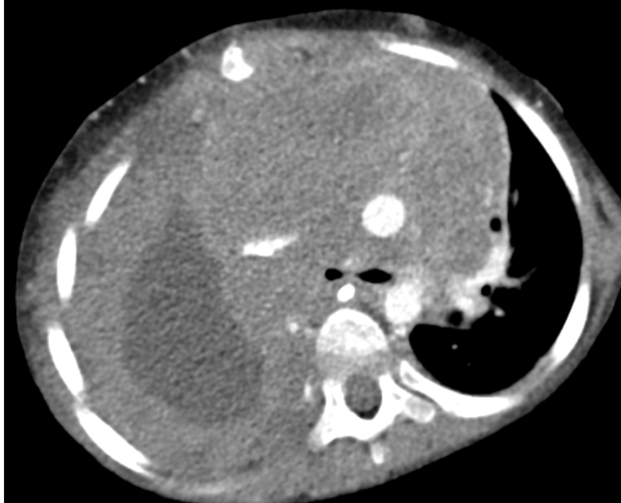

80 kVp

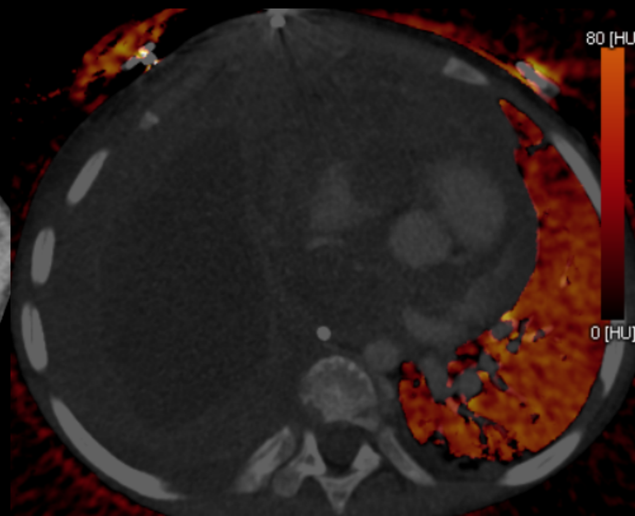

Perfusion Image

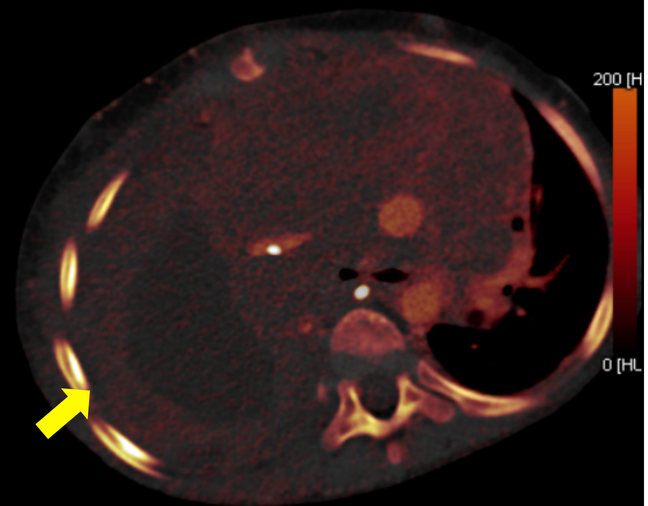

Iodine Map

3-year-old female with right pleuropulmonary blastoma, status post right pneumonectomy. There is no perfusion in the right lung status post pneumonectomy. There is iodine material in the thickened soft tissue in the periphery of right chest, consistent with recurrent tumor (arrow).

Urinary Tract Stone Characterization

Uric acid stones can be treated conservatively with alkalization of urine. However, calcium stones need to be removed or broken into small pieces.

- Uric acid stones: increased photon attenuation at 140 keV because the attenuation is driven primarily by Compton scatter (due to lighter element chemical composition)
- Non-uric acid stones: increased attenuation at 80 keV due to increased photoelectric effect contribution from the heavier elements nearing the k-edge of calcium (4 keV)

Renal stone characterization

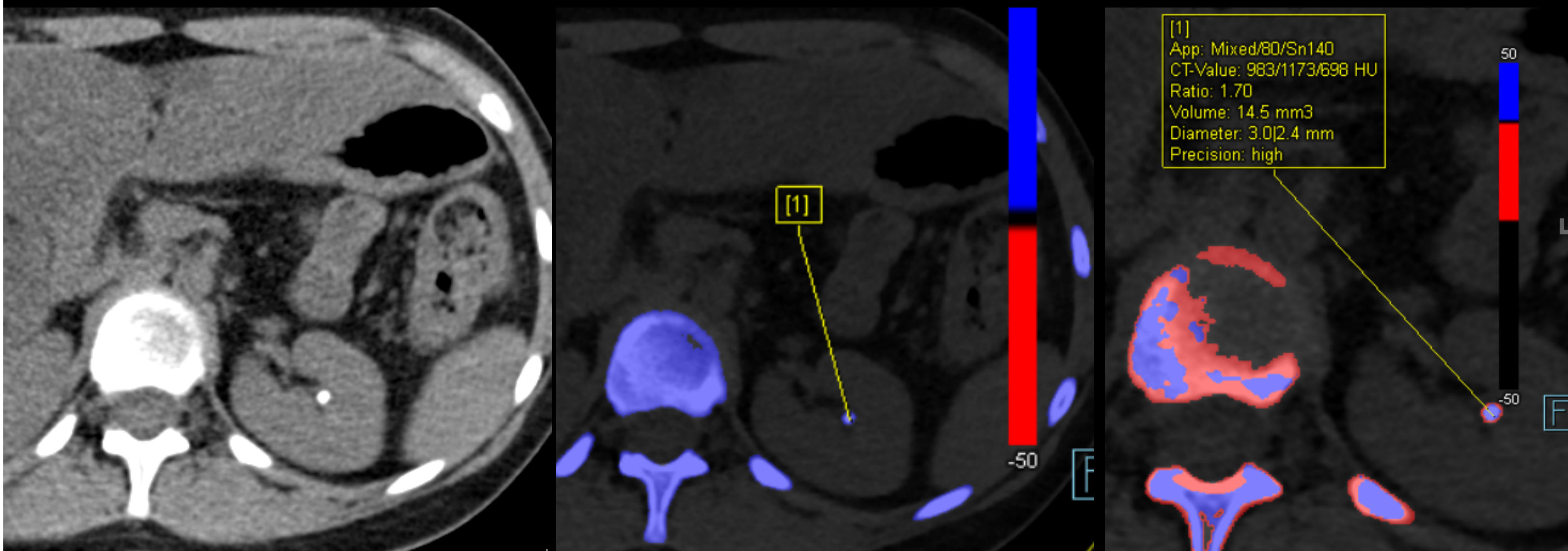

19-year-old female with cystic fibrosis and a renal stone. Ratio of low to high energy attenuation is 1.7, highly suggestive of a calcium stone (color coded as blue by default).

Renal stone characterization

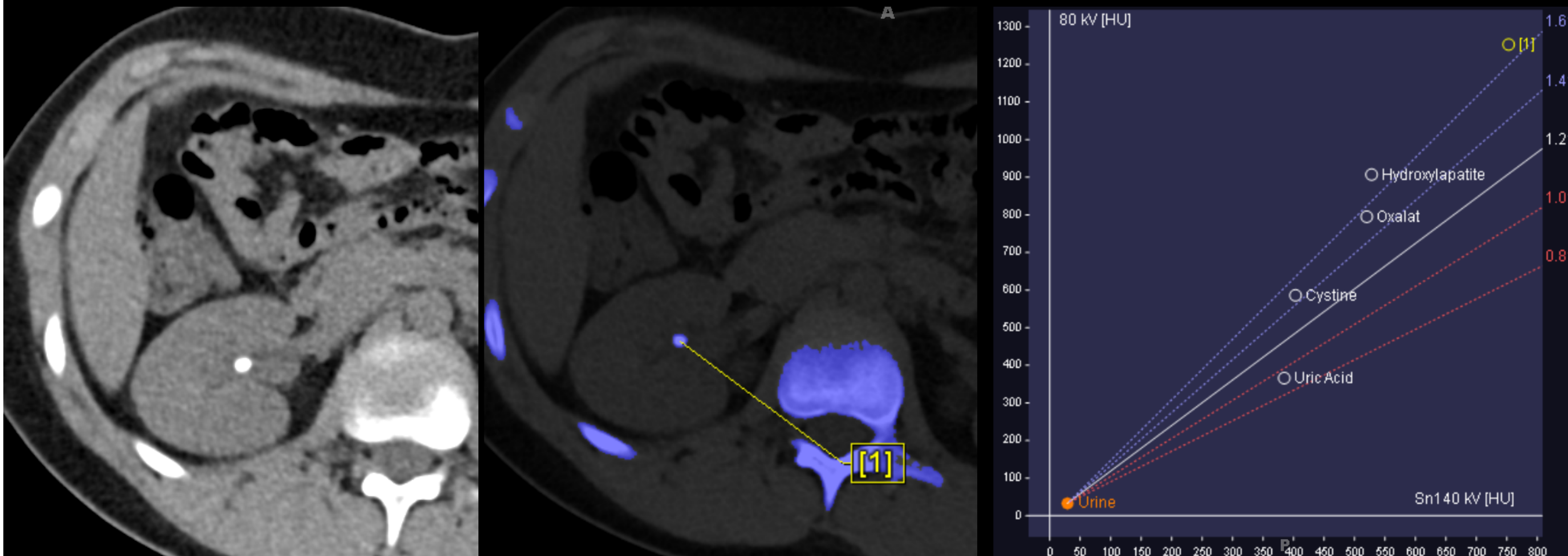

14-year-old female with nephrolithiasis. Ratio of low to high energy attenuation is above 1.6, highly suggestive of a calcium stone.

Automated Bone Subtraction

- Dual energy Subtraction
  - Material differentiation of iodinated contrast and calcium
  - Based on the characteristic attenuation behavior of iodine and calcified bone at high and low photon energies
- Traditional CT Subtraction
  - Threshold based segmentation

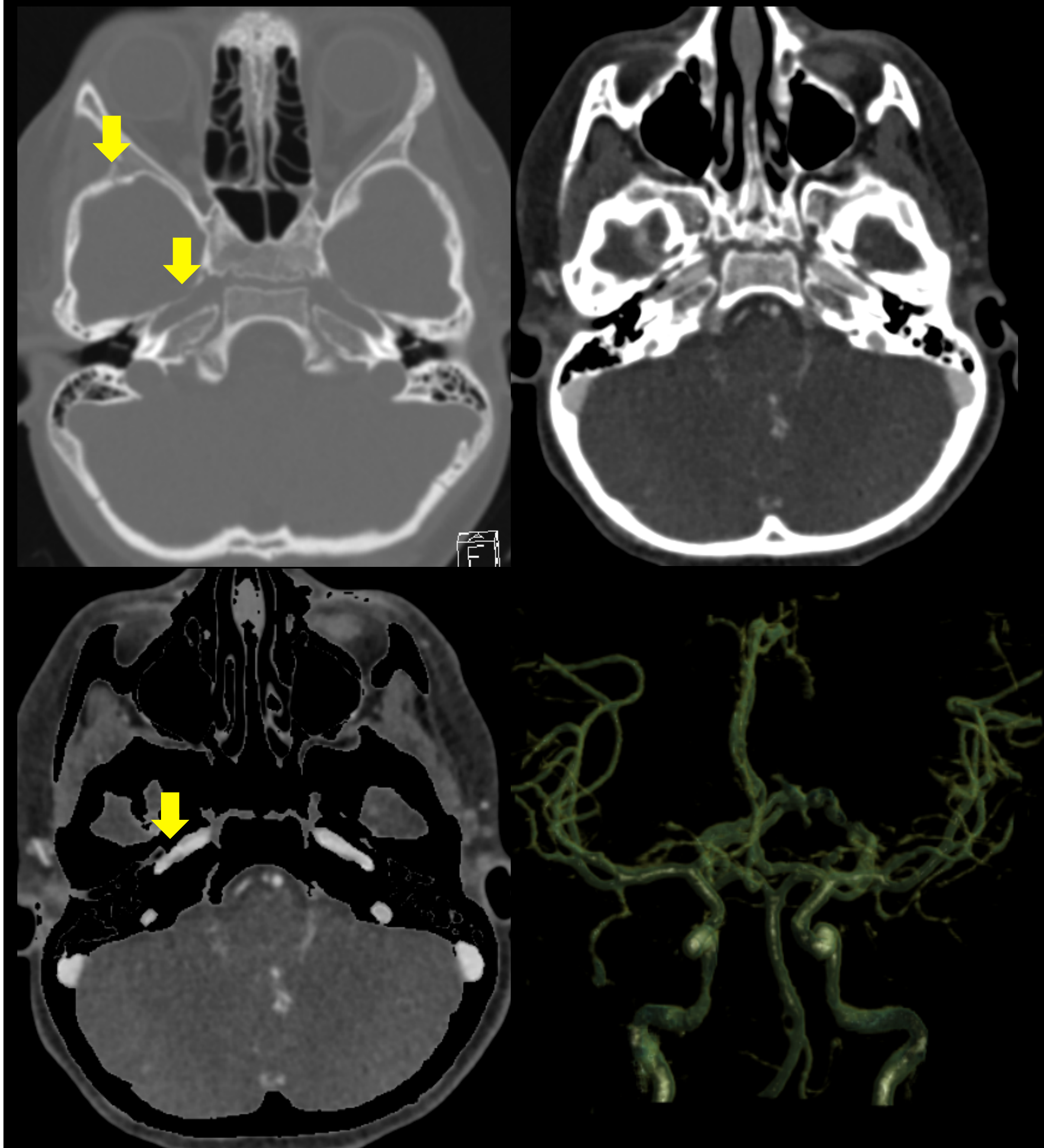

Automated Bone Subtraction

6-year-old boy with sledding injury.

- Skull base fracture involving the right greater sphenoid wing extending into the petrous portion of the right internal carotid canal.
- CTA was performed to evaluate vessel integrity. Visualization of petrous portion of the ICA is challenging due to complex bony structure of skull base.
- Automated bone subtraction improves visualization of the vessel. There is narrowing of the petrous portion of the right internal carotid artery at the level of the fracture, likely arterial vasospasm.

CTA with Automated Bone Subtraction

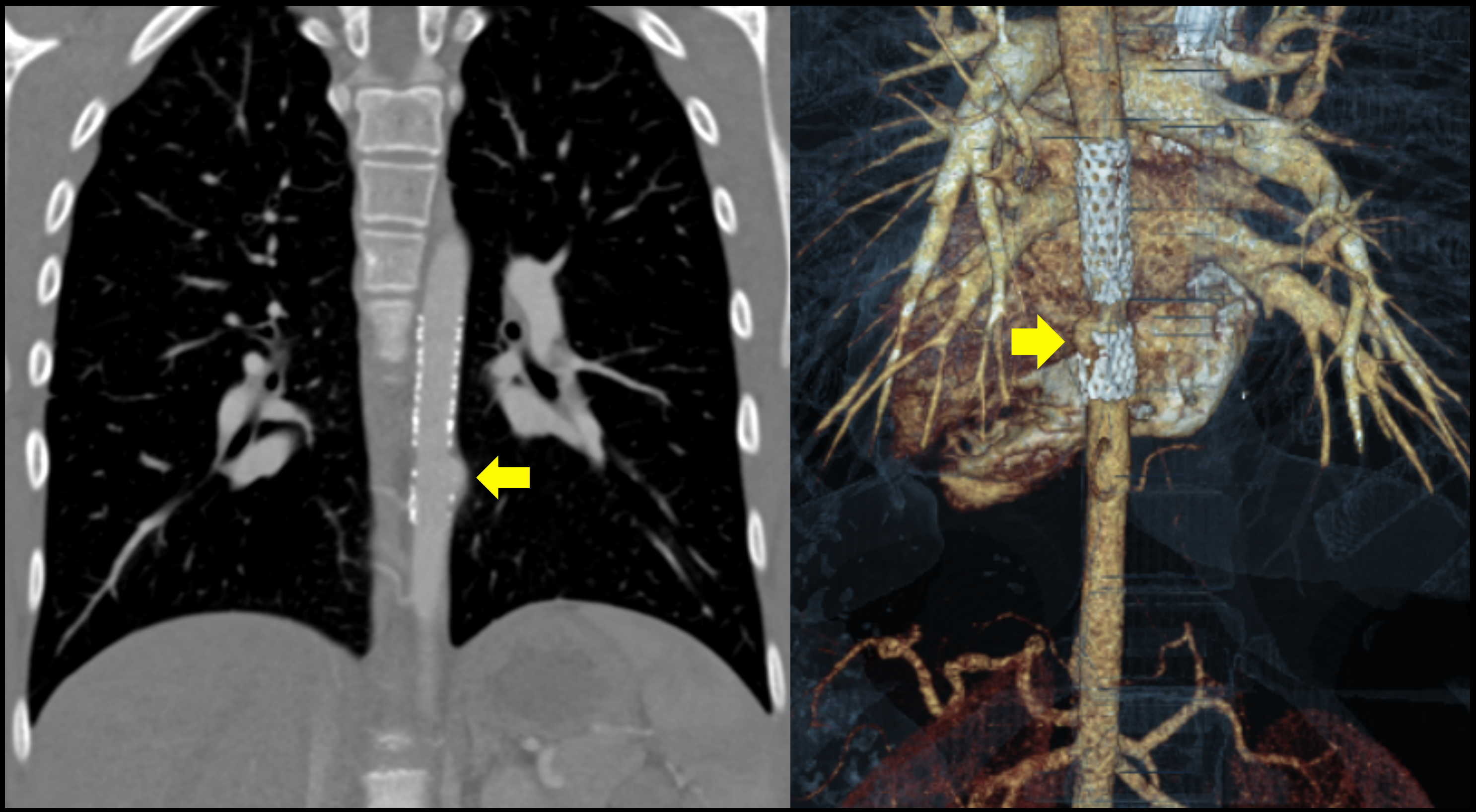

13-year-old female with Takayasu arteritis and middle aortic syndrome status post balloon dilation and stent. There is stent fracture and focal outpouching through the stent gap on the left. VRT 3D reconstruction with bone removal better visualizes the fracture and the aneurysm (posterior view).

“Easy” 3D Reconstructions

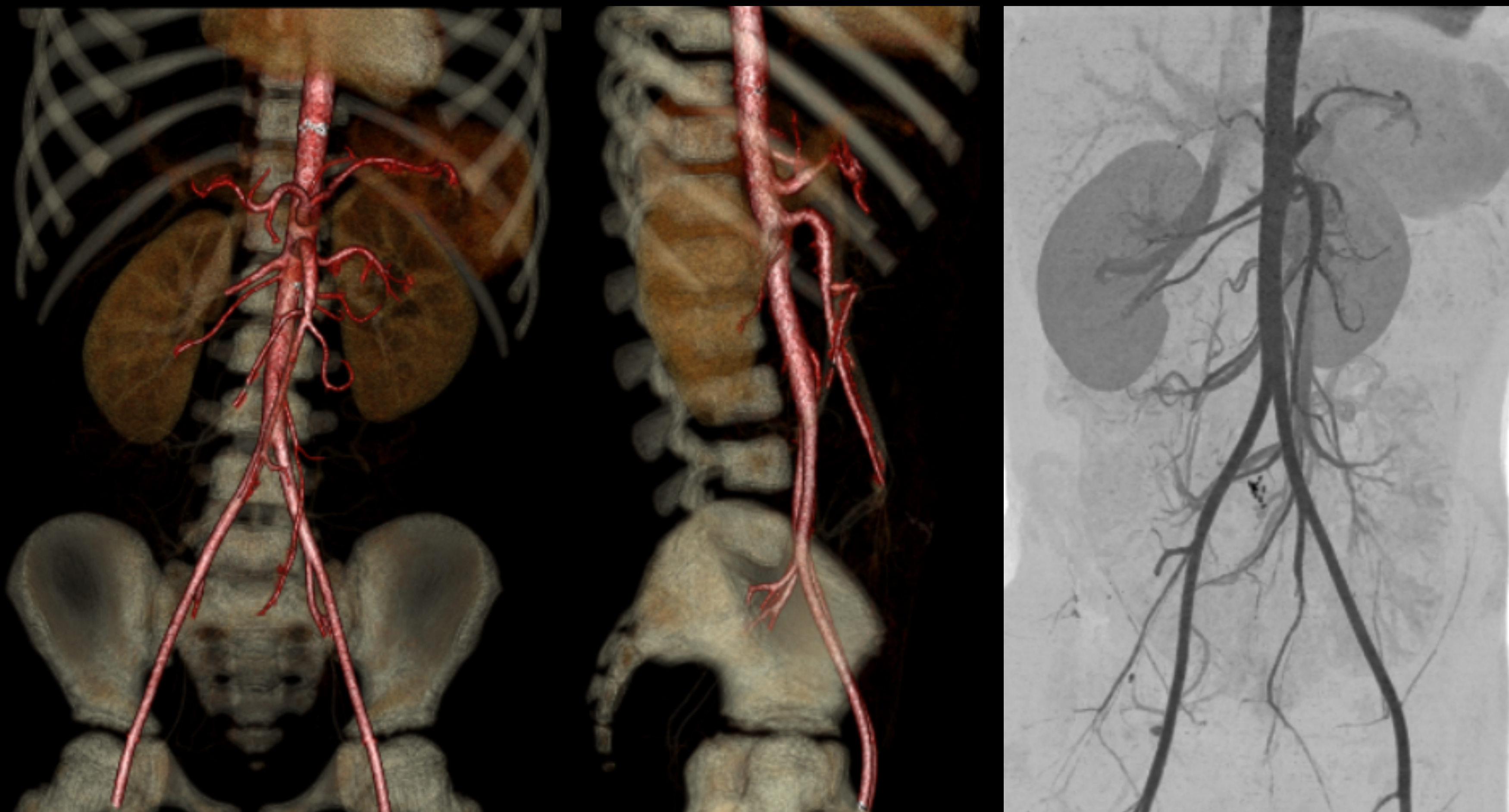

12 year old male with cystic fibrosis and recent colitis; normal CT angiogram of the abdominal aorta. Surface-shaded volume rendered 3D reconstructions are simple to create with DECT datasets with varying levels of opacity in nonvascular structures or complete bone removal (*right*, MIP image).

Conclusion

DECT provides “multiple studies in one” and can improve diagnosis and characterization of diseases in the pediatric population *without additional radiation exposure*

References

1. Johnson TRC. Physics of dual-energy CT. *https://www.DSCT.com*. Posted on Dec 21, 2009. Accessed 25-Feb-2017.

2. Siegel MJ, Curtis WA, and Ramirez-Giraldo JC. Effects of dual-energy technique on radiation exposure and image quality in pediatric body CT. *AJR* 2016; 207:1-10.

3. Siegel MJ, Ramirez-Giraldo JC, and Graser A. Abdominal dual-source dual-energy CT: uses in clinical practice. *Applied Radiology* 2013; 11:10-16.